Echo-Planar Spin-Echo and Inversion Pulses

John Pauly, Dan Spielman, Albert Macovski

The echo-planar *k*-space trajectory can be used as the basis for any two-dimensional selective pulse. The main application is spectral-spatial pulses, which must be based on the echo-planar trajectory. In this paper we show how echo-planar spin-echo (EPSE) pulses may be designed.

Key words: RF pulse design; multidimensional pulses; spectral-spatial pulses.

INTRODUCTION

Echo-planar *k* trajectories have been used for the acquisition phase of MR imaging for many years (1). The first application to selective excitation was by Meyer *et al.* (2) in the design of two-dimensional pulses that are simultaneously selective in the spectral dimension and one spatial dimension. Only those spins in a given range of chemical shift frequencies *and* a given slice are excited. The chemical shift evolves at a constant rate with time, not under gradient control. The 2D *k* trajectory with one constant axis is the conventional echo-planar trajectory. For spectral-spatial pulses there is no other choice.

The primary application for echo-planar spin-echo (EPSE) pulses has been in metabolite imaging (3, 4). For example, the SIMPLE pulse sequence uses a spatially selective two-dimensional excitation and an EPSE refocusing pulse provide 3D spatial localization and water suppression in a two pulse spin-echo sequence (3).

Multi-dimensional large-tip-angle pulses, such as spin-echo pulses, can be designed using Fourier transform arguments provided the *k*-space trajectory and RF weighting satisfy certain symmetry constraints (5). Unfortunately the echo-planar trajectory does not fall within this class. Echo-planar spin-echo pulses designed this way do work, but the actual profile differs substantially form the desired profile.

Multi-dimensional adiabatic pulses have been designed by first taking a spectral adiabatic hard pulse sequence, and replacing each hard pulse with spatially selective subpulses (6). In this case all subpulses should have the same slice profile, each scaled to the appropriate tip angle. EPSE pulses can also be designed this way (7). These pulses work better than the Fourier designs, but still suffer some slice profile distortion.

MRM 29:776–782 (1993)

From Magnetic Resonance Systems Research Laboratory, Department of Electrical Engineering (J.P., A.M.), and Lucas Center for Magnetic Resonance Spectroscopy and Imaging, Department of Radiology (D.S.), Stanford University, Stanford, California.

Address correspondence to: John Pauly, Ph.D., Durand 105A, Stanford University, Stanford, CA 94305.

Received November 23, 1992; accepted December 15, 1992.

This work was supported in part by National Institutes of Health (Grants HL-39478, HL-39297, HV-38045, HL-34962, NCI-CA 50948, and NCI-CA 48269) and the Lucas Foundation.

0740-3194/93 $3.00

In this paper we propose a better approach. The key idea is that at each spatial location we need to simultaneously apply different spectral pulses. In the next section we examine what this means, and how it can be accomplished.

EPSE DESIGN

Decomposition into Subpulses

EPSE pulse design is based on the decomposition of the full 2D pulse into a sequence of simple 1D subpulses. These subpulses are inherently refocused pulses (IRPs), which perform pure rotations about the applied RF. Echo-planar pulses can be considered to be the concatenation of a sequence of IRP's. This viewpoint helps explain the unusual refocusing requirements of EPSE pulses.

An inherently refocused pulse consists of a gradient and RF waveform that together produce a Hermitian symmetric *k*-space weighting (8), where the spatial frequency variable is defined

$$k(t) = \gamma \int_t^0 G(s)ds.$$

This is the integral of remaining gradient from the time t until the end of the pulse. A small-tip-angle IRP produces a rotation about the RF axis. The rotation angle is proportional to the Fourier transform of this weighting,

$$\theta(x) = \gamma \int_{-T}^{0} B_1(t)e^{ix \cdot k(t)}dt, \qquad [1]$$

where the pulse starts at time $-T$ and ends at zero. For example, if the RF is applied along the x axis, the IRP produces a rotation about x. The tip angle varies as a function of position, but the rotation axis is everywhere the same. This is true for any initial or final magnetization.

For our current purposes we only need a very simple one dimensional IRP, illustrated in Fig. 1a. This consists of a prefocusing gradient lobe of area one-half, a conventional slice-selective RF pulse along with a constant gradient of area one, followed by a refocusing gradient lobe of area one-half. Fig. 1b shows the *k*-space trajectory and RF weighting. The rotation angle produced by this pulse is the Fourier transform of this weighting, shown in Fig. 1c.

As in the design of 2D adiabatic pulses, we can concatenate a sequence of 1D IRP's to form a 2D echo-planar type pulse (6). One segment of such a pulse is shown in Fig. 2a. As in (6) we invert the gradient for every other IRP. The prephase and dephase lobes cancel and can be omitted, allowing the RF pulses to be much more closely spaced, as shown in Fig. 2b.

This produces the unusual refocusing properties of these pulses. All of the prephase and rephase gradients

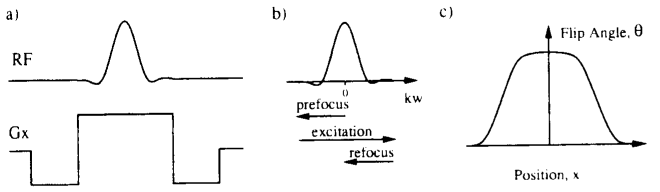

FIG. 1. Simple one-dimensional inherently refocused pulse (IRP) consisting of both prefocusing and refocusing gradient lobes surrounding a conventional slice-selective pulse (a). The *k*-space trajectory is shown in (b), and the tip angle profile in (c).

lobes cancel, except for the first and last. The number of IRPs may be either even or odd. The case of an even number of IRPs is shown in Fig. 3a. If the full concatenated pulse is a spin-echo pulse we can move a gradient lobe from one end of the pulse to the other by inverting its sign. This means we can have a spin-echo pulse that is either only prefocused (Fig. 3b) or refocused (Fig. 3c). The case of an odd number of IRPs is shown in Fig. 3d. Here when we move either gradient lobe to the other end, the two cancel, Fig. 3e. It would appear that this is the most desirable case. In practice, however, the spin-echo pulse will be surrounded by crusher (dephasing) gradients. The prefocus and refocus gradients can then be incorporated into the crusher gradient areas. It should be noted that all these prefocus and refocus combinations are the same only for the spins inside the slice. For spins outside the slice these have quite different effects. The variations with both prefocusing and refocusing lobes (Fig. 3a,d) have zero total gradient area, so the out-of-slice spins are left totally unaffected by the pulse. They are not flipped at all by the RF or dephased by the gradient. The others have non-zero gradient area, so the out-of-slice spins are at least somewhat dephased by the action of the gradient during the pulse.

Gradient Waveforms

So far we have assumed that the oscillating echo-planar gradient waveform is an ideal square wave. In practice this is far from true. Usually the gradients are slew-rate limited, so realizable gradient waveforms consist either largely or entirely of ramps. In order to use nonconstant gradient waveforms the RF subpulses must be compensated to produce the correct *k*-space weighting, in accordance with the VERSE idea (9). Fig. 4a is a plot of the ideal square wave gradients. Fig. 4b is a plot of a triangle gradient waveform, which is optimal when gradient slew rate is the only constraint. If gradient amplitude is also a constraint the optimal waveform is trapezoidal, Fig. 4c. Peak RF amplitude is sometimes the limiting constraint for EPSE pulses designed for spatial slab-select pulses with sharp profiles. In this case the gradient can be dropped at the center of the subpulses to reduce the peak RF, as in (6). This is illustrated in Fig. 4d. In (6) a loss in gradient area of about 12% permitted the peak RF amplitude to be halved.

One additional concern is the difference between the types of echo-planar trajectories. For spectral-spatial pulses the *k*-space trajectory moves at a constant rate along the spectral axis, while oscillating in the direction

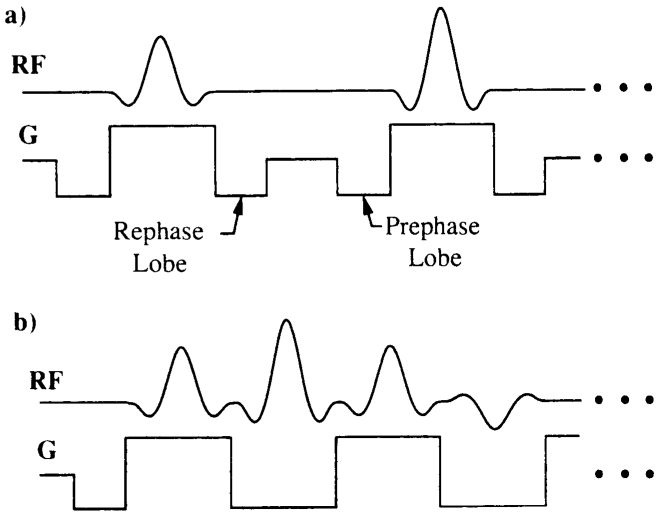

FIG. 2. Synthesis of a 2D EPSE pulse from IRP's. In (a) the IRPs of Fig. 1 are simply concatenated. Inverting the gradient for every other IRP allows the interior prephase and rephase lobes to cancel, and the whole pulse to be shortened. The initial prephase lobe and the final rephase lobe (not shown) don't cancel, and must be included.

of the spatial axis. Gradient waveforms and the corresponding *k*-trajectory are plotted in Fig. 5a and b. This is the conventional echo-planar trajectory. In designing EPSE pulses we will assume that the spectral evolution happens in a blip between the IRP subpulses, illustrated in Fig. 5c and d. This corresponds to the blipped echo-planar trajectory, which is easier to analyze. This assumption produces some error in the design which increases with spectral frequency (2). In practice we are only concerned with the main-lobe and first nulls of the profile, where the approximation is reasonably good. The effects of this approximation will be demonstrated in the example designs presented below.

The approximation is always perfect at one spectral frequency, the origin. At this point there is no spectral phase shift between subpulses, so it doesn't matter

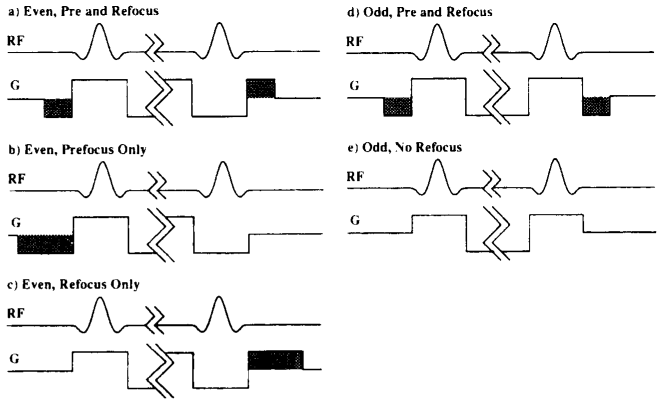

FIG. 3. Different prefocus/refocus possibilities for EPSE pulses. An even number of subpulses (a–c) allows either prefocusing (b), refocusing (c), or both (a). With an odd number of subpulses (d–e) the possibilities are both (d) or neither (e). In the last case the prefocusing and refocusing lobes cancel when moved from one end of the pulse to the other.

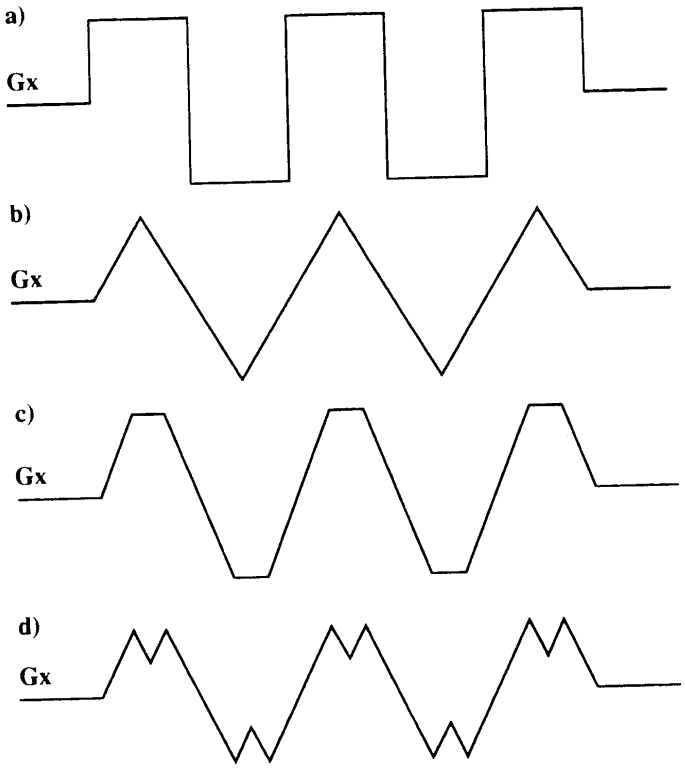

FIG. 4. Gradient waveform considerations. The ideal waveform for the oscillating gradient is shown in (a). This requires infinite gradient slew rates. The triangle gradient waveform (b) produces the maximum *k*-space coverage when gradient slew rate is the only constraint. When peak gradient amplitude is also a constraint the waveform becomes trapezoidal (c). One unfortunate aspect of the waveform in (b) is that the RF amplitude at the *k*-space origin is maximized. If peak RF amplitude is also a constraint the gradient can be reduced in the middle to allow the RF amplitude to be brought down, as in (d).

whether the spectral shift is constant or blipped. This is useful for designing very high quality rejection bands for water suppression, as we will show below.

2D Inverse SLR Transform

The idea behind the design of spectral-spatial EPSE pulses is that at each spatial position we would like to apply a different spectral hard pulse sequence. Inside the slice we want a 180° rotation, outside the slice we want a 0° rotation. In the transition band all of the intermediate rotation angles must occur. All of these different pulses must be applied simultaneously.

We start by choosing an echo-planar gradient trajectory. There are two major constraints. First, the area of each gradient lobe determines the extent of the k_x coverage, and hence the minimum slice width. This is improved by using longer gradient lobes. The other constraint is the location of the replication sidelobes in the spectral dimension. Major sidelobes occur at multiples of the oscillating gradient frequency. In addition there are asymmetric "ghost" sidelobes halfway between the major sidelobes (2). The gradient frequency must be high enough to ensure that these sidelobes are beyond the edge of the spectral stop band. For example, if we use 1 ms gradient subpulses with a total pulse duration of 16 ms we can obtain a slice thickness on the order of 1 cm, while the nearest sidelobes are centered at ±500 Hz.

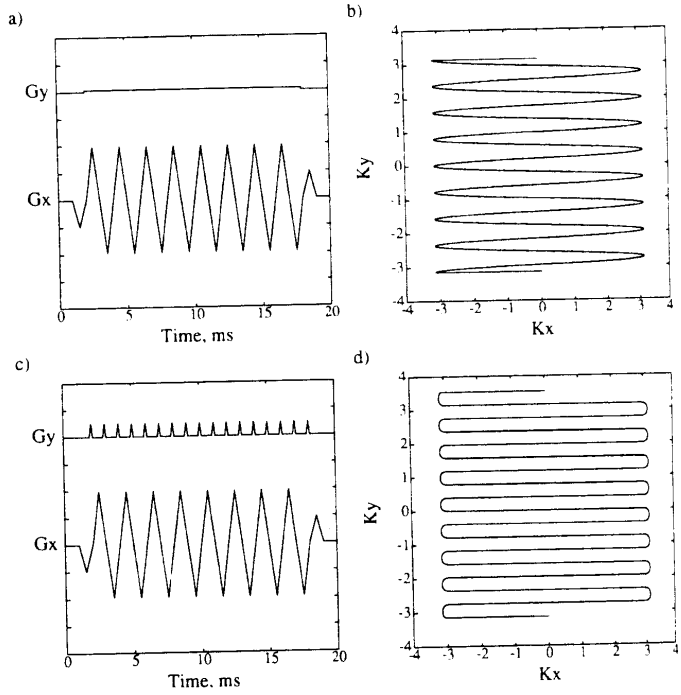

FIG. 5. Different types of slew-rate limited echo-planar trajectories. (a) and (b) are the conventional (constant slow gradient) echo-planar gradient waveforms and *k*-space trajectory. This is necessarily the trajectory for EPSE pulses. (c) and (d) are the blipped echo-planar gradient waveforms and *k*-space trajectory. This is the model we assume when designing EPSE pulses.

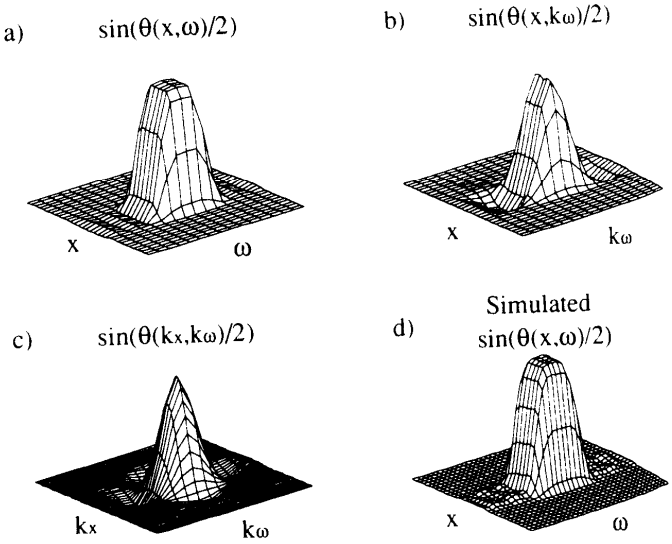

FIG. 6. Stages of the two-dimensional inverse SLR transform. The input to the 2D inverse SLR transform is shown in (a). After the first one-dimensional inverse SLR transform along the spectral dimension (b) the surface can be considered to be the spatial profiles as a function of the subpulse index. (c) is the result of the inverse SLR transform along the spatial dimension. The RF pulse is computed by traversing this surface in the raster echo-planar manner. The RF pulse and the spin-echo profile are shown in Fig. 7. The response produced by this pulse is shown in (d). This agrees well with the desired response (a).

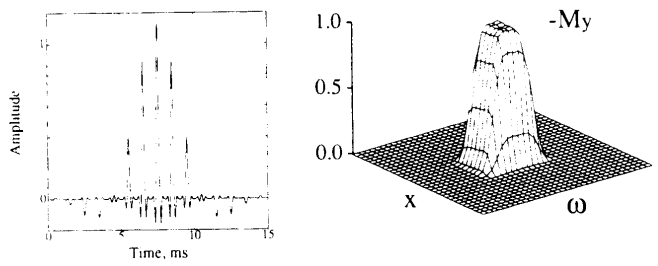

FIG. 7. RF pulse produced by tracing the surface of Fig. 6c in the raster echo-planar trajectory (a), and the crushed spin-echo profile this pulse produces (b). The sidelobes are lower than in Fig. 6d due to the square dependence on flip-angle.

Next we choose the 2D profile we would like to produce. Ideally we would like to specify the rotation. Practically it is easier to specify the Cayley-Klein spin parameter $\beta(x,\omega)$, which is

$$\beta(x,\omega) = i(n_y - in_x)\sin(\theta(x,\omega)/2)$$

where $\theta(x,\omega)$ is the flip angle at a particular position and spectral frequency, and $(n_x, n_y, 0)$ is the unit vector defining the axis of the rotation (10). The crushed spin-echo profile is

$$M_{xy}(x,\omega) = i\beta^2(x,\omega)$$

for spectral-spatial pulses it is usually easier to design the 2D profile as the product of two 1D profiles, although this is not necessary. The spectral and spatial profiles can be designed by any method, such as Fourier design or by digital filter design methods. The usual pulse design constraints apply. For example, the bandwidth of the spatial profile profiles determines the minimum slice width. In the spectral dimension the β must be the Fourier transform of a discrete sequence of the same length as the number of subpulses. The 2D profile is simply the outer product of the two 1D profiles. Fig. 6a is a plot of the initial $\beta(x,\omega)$ specified for the design of an EPSE pulse.

The calculation of the RF waveform proceeds in two stages. Conceptually we can consider this process to be a 2D inverse SLR transform, similar in idea to a 2D inverse discrete Fourier transform. A major difference is that the order of the transforms is critical in the SLR case. A formal derivation of the inverse SLR transform for two dimensions has been reported by Buonocore (11). Here we proceed by considering how the spatially selective subpulses and the spectrally selective envelope interact.

The first stage consists of 1D inverse SLR transforms (10, 12, 13) along the spectral dimension. These are computed for each spatial position along the uniformly sampled spatial dimension. The flip angle at each position is determined by the spatial profile. Inside the slice the flip angle is π, in the transition band it varies continuously from π down to close to zero, and out-of-slice it stays close to zero. This is important because of the "bandwidth narrowing" effect of large flip angle pulses which causes the slice profile to be significantly narrower than the frequency content of the pulse would indicate. This means that a π pulse must have a wider bandwidth to have the same slice width as a $\pi/2$ pulse. This first stage of the EPSE design insures that at each spatial position the spectral hard pulse has the appropriate bandwidth. Fig. 6b shows the result of this first transform stage applied to the initial specification plotted in Fig. 6a. Close inspection shows the in-slice pulses are narrower than the transition band pulses, illustrating the compensation for large-tip-angle bandwidth narrowing.

The second stage consists of 1D inverse SLR transforms in the spatial dimension. The first stage has computed the spectral hard pulses that must be played at each spatial position. In the second stage we compute each of the spatial subpulses. Consider the j^{th} sample of all of these spectral hard pulse sequences. Taken together this is the flip-angle profile that must be produced by the j^{th} spatial subpulse. These are generally relatively small flip angles, in which case they can be designed using Eq. [1]. For

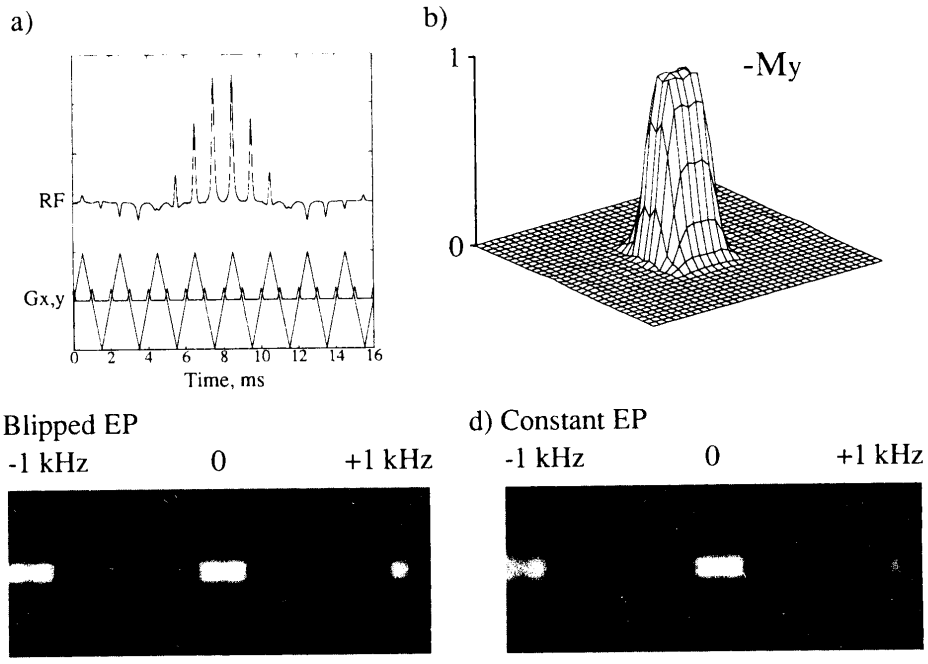

FIG. 8. Example of a linear-phase spectral-spatial pulse designed for water-lipid selection. The RF pulse is plotted in (a), and the simulated M_y crushed spin-echo profile in (b). Experimental profiles are shown for the blipped slow gradient in (c) and a constant slow gradient in (d). The constant gradient profile is equivalent to the spectral-spatial response.

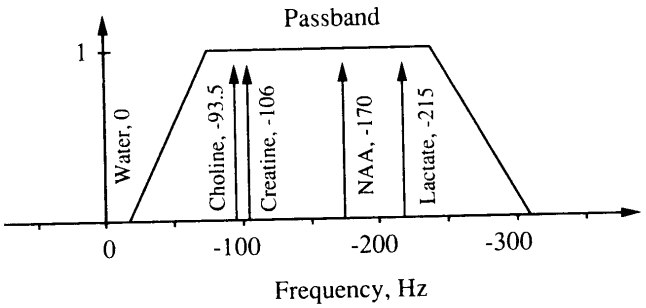

FIG. 9. Pass and stopband locations for the metabolite imaging EPSE pulse. Also shown are the spectral locations of several of the key metabolites. The band edges were chosen assuming a B_0 inhomogeneity of 26 Hz peak-to-peak.

larger flip angles or more accurate designs the SLR algorithm should be employed, again using the relation that $\beta(x) = i(n_y(x) - in_x(x))\sin(\theta(x)/2)$, where $(n_x(x), n_y(x), 0)$ is the axis of the rotation at a particular spatial position.

Fig. 6c is the result of applying the 1D inverse SLR transforms to the spatial dimension of the function in Fig. 6b. The EPSE RF waveform is found by tracing this surface along the raster echo-planar trajectory. The response produced by this RF pulse is shown in Fig. 6d. The agreement with the desired response, Fig. 6a, is very good. The RF pulse itself and the spin-echo profile are plotted in Fig. 7. Note that the subpulses in Fig. 7 differ both in amplitude and in shape.

Most spin-echo pulses are designed to have linear phase, meaning that at the time of echo formation all refocused spins are in phase. This is important for imaging where the integral across the profile is of concern. In spectroscopy this is not the case. The spectral profile is subsequently resolved. Any known spectral phase profile can be corrected. Substantial spectral profile improvement can be obtained by exploiting this flexibility in phase profile (10). This will be demonstrated in the next section where we present design examples.

DESIGN EXAMPLES

We will consider two design examples here. The first is a linear-phase EPSE pulse suitable for imaging either the water or lipid peak while suppressing the other. This is similar to the example of the previous section. The second is a higher performance pulse designed particularly to provide water suppression for metabolic imaging (3, 4). Here we want very high stop-band attenuation over a narrow band about at the water frequency, and very sharp transition between the pass and stop bands. We use a minimum phase pulse, designed with the water stopband on resonance.

Linear-Phase EPSE Pulse for Lipid-Water Imaging

The first example is a linear-phase EPSE pulse. In the spectral dimension we choose a time-bandwidth product $TB = 4$ profile. If we use a 16 ms pulse the bandwidth is 250 Hz, from ± 125 Hz. The transition width depends on the ripple allowed in-slice and out-of-slice (10). If we make the passband ripple 1% and the stopband ripple 0.1%, then the figure of merit D_∞ for the pulse is 2.0 (see ref. 10). The transition band is then $250 \cdot 2/4 = 125$ Hz, going from 62.5 Hz to 187.5 Hz. At 1.5 T the water-lipid difference frequency is about 230 Hz, so the stopband and passband widths allow on the order of ± 1 ppm tolerance to B_0 inhomogeneity. The sampling rate determines the separation between the main lobe and the sidelobes. We choose this to be 1 kHz, so the subpulses are

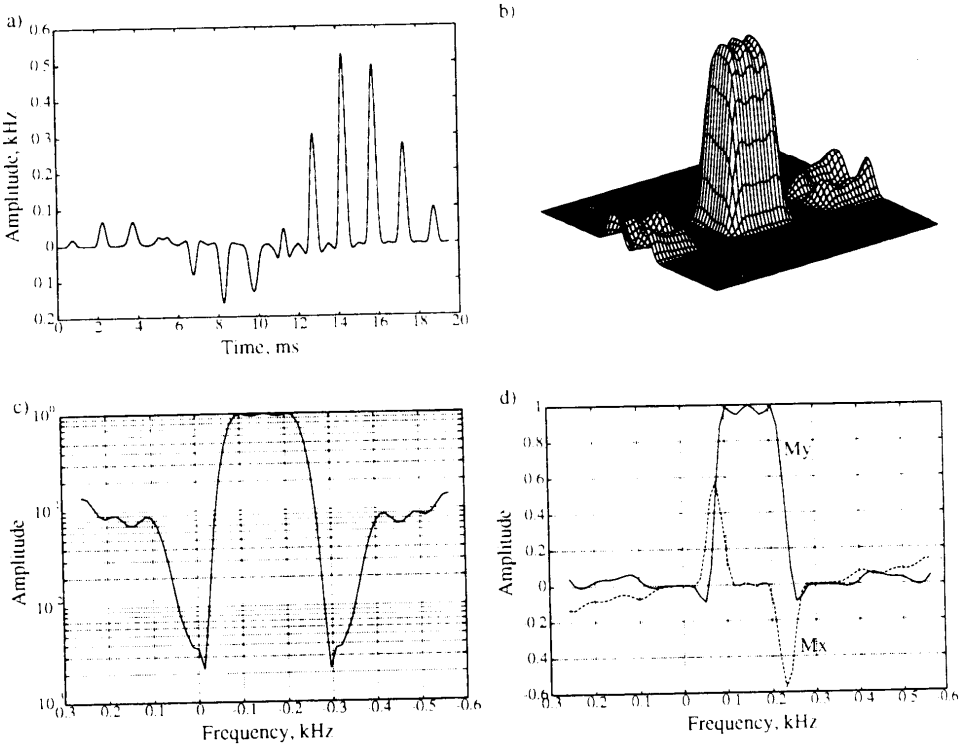

FIG. 10. Minimum phase spectral-spatial EPSE pulse designed for metabolite imaging. The basic design is plotted in (a), along with the spectral-spatial profile (b). (c) a logarithmic plot of the spectral profile after integrating over the spatial dimension. Note that the stopband at zero, where water will be, is fairly deep, but not very broad. The M_x and M_y profiles are plotted in (d) to illustrate the nature of the phase shifts caused the minimum phase profile. The phase is zero over most of the passband. It does shift at the edges of the passband, but is spectrally resolvable and can readily be corrected on reconstruction.

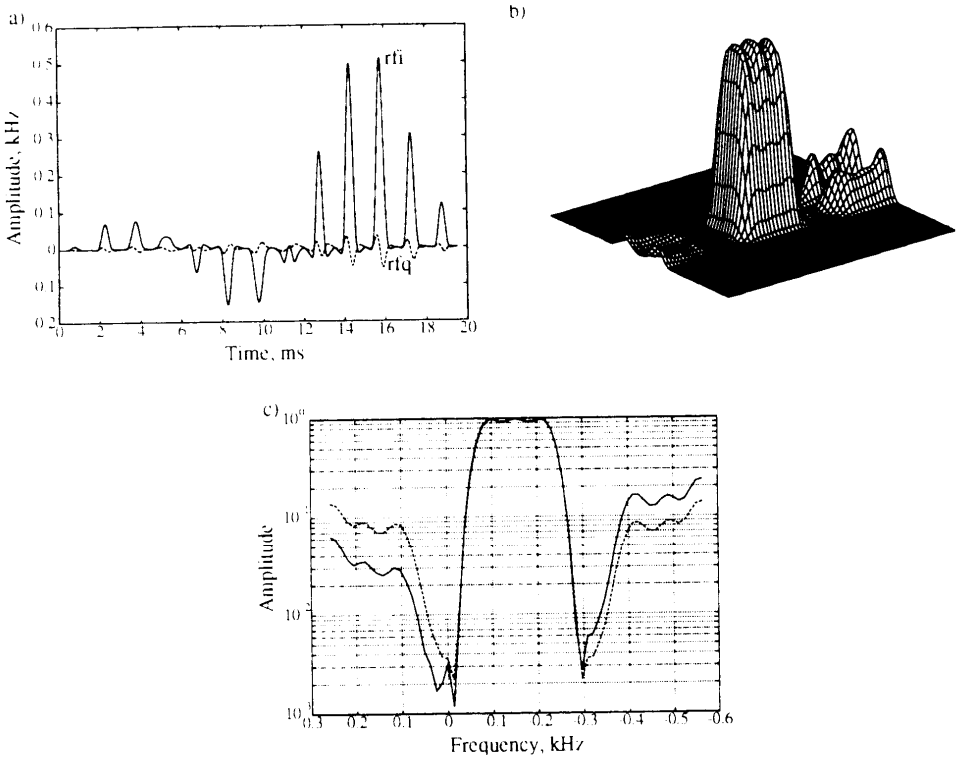

FIG. 11. EPSE pulse designed with the stopband on resonance, and then modulated. The pulse (a) is very similar to that in Fig. 10a, differing mainly in the presence of a small quadrature component. The profile has a reduced sidelobe near the critical stopband, while the other sidelobe has increased. A comparison of the spectral profiles after integrating across the spatial dimension shows that the on-resonance stopband is both broader and deeper.

each 1 ms in duration. This puts the first ghost sidelobes at ±500 Hz, which is far enough away not to contaminate the first stopbands.

In the spatial dimension we choose a $TB = 2$ profile. For convenience we use Dolph-Chebyshev window profile (14). The gradient is a triangle waveform. Each lobe is 1 ms long, so at a gradient slew rate of 2 (G/cm)/ms the gradient just reaches the 1 G/cm full scale on our 1.5T GE Signa system. The maximum excursion in k_x is then about ±1 cycle/cm. With a time-bandwidth 2 profile this gives a minimum slice width of about 1 cm.

The pulse with these specifications is plotted in Fig. 8a. The simulated crushed spin-echo profile is plotted in Fig. 8b. Images of experimental profiles are shown in Fig. 8c and d. Fig. 8c is the profile obtained with the blipped slow gradient assumed in the pulse design. Fig. 8d is the experimental profile for a constant slow gradient, which simulates the spectral-spatial response. Note the presence of the "N/2" ghosts centered at ±500 Hz.

Minimum-Phase EPSE Pulse for Metabolic Imaging

The next example is of pulse specially designed for a multislice metabolic imaging pulse sequence (4). Most of the water suppression in the sequence is from the EPSE pulse, so the quality of the spectral stopband is critical. The constraints on the spectral profile are determined by the location of the metabolites of interest and B_0 homogeneity. We assume a B_0 inhomogeneity of 26 Hz peak-to-peak. If the water frequency is taken to be zero, the stopband goes from ±13 Hz. The metabolite closest to water is choline, which is at −93.5 Hz, so the lower passband edge is at −80.5 Hz. Fig. 9 is a plot of the pass and stop bands, along with the location of several of the important metabolites.

Unless overridden, our 1.5T GE Signa (GE Medical Systems, Milwaukee, WI) enforces an RF pulse length limit of slightly less than 20 ms. With 1.5 ms subpulses, 13 subpulses fit in 19.5 ms. The major replication sidelobes are offset from the main lobe by 666 Hz, and the ghost sidelobes by 333 Hz. This is enough separation to preserve the required 26 Hz stopbands. The gradient sublobes will be trapezoids since full amplitude can be reached in 0.5 ms. The maximum excursion in k space is then about ±2 cycles/cm, allowing 1 cm slices with a sinc-cycle 1 (time-bandwidth 4) profile.

The spectral profile has a bandwidth of 215 Hz, a transition width of 66.6 Hz, while the overall pulse duration is 19.5 ms. The effective duration of the pulse is the time between the centers of the first and last subpulses, which is 18 ms. The "quality factor" D_∞ for this profile (10) is

$$D_\infty = TBW$$

$$= (18 \cdot 10^{-3}\text{s})\,(215\text{ Hz})\left(\frac{66.6\text{ Hz}}{215\text{ Hz}}\right)$$

$$= 1.2$$

which is quite small for a spin-echo pulse. This is a difficult profile to achieve. There are two parameters to be chosen, the passband ripple and the stopband ripple. The passband ripple should be smaller than the expected noise level. Here we choose the passband ripple to be 5%, so noise will be the limiting factor until an SNR of 20, which is very high for metabolite images. If we use a linear phase profile the minimum stopband ripple is about 2%, which is entirely inadequate. However, if we go to a minimum phase profile the minimum obtainable stopband ripple drops to 0.1%. Using a minimum phase profile increases the stopband attenuation by a factor of 20, which is a very substantial improvement.

The EPSE pulse designed to these specifications is shown in Fig. 10a, and the simulated spin-echo spectral-spatial profile in Fig. 10b. The spectral phase profile is plotted in Fig. 10d. The phase dispersion from the minimum-phase pulse occurs principally at the edges of the passband, and varies slowly relative to normal spectroscopic resolution. Since the phase is known and resolvable, it can be corrected on reconstruction.

This pulse was designed with the center of the passband on resonance, so at this frequency the profile is undistorted by the effects of the difference between the blipped EP trajectory assumed in the design and the continuous EP trajectory inherent in a spectral-spatial pulse. Unfortunately, the part of the profile that we care about most is the stopband. If we look at the logarithmic plot of the integrated spectral profile in Fig. 10c we see that the stopband is fairly deep, but that the first sidelobe is interfering. The result is that the stopband is much narrower than desired.

The fidelity of the stopband can be improved by initially designing the EPSE pulse with the stopband on resonance. After the pulse has been designed it can be shifted by modulation (simulating a change in center frequency). The RF pulse produced by this method is plotted in Fig. 11a, and its profile in Fig. 11b. The pulse is very similar to that in Fig. 10a, differing mainly in the presence of a small quadrature component. The difference in profile is substantial, though. The sidelobe near the design frequency is reduced, while the other sidelobe increases. Logarithmic plots of the integrated spectral profile (c) shows that the stopband at the designed frequency is both broader and deeper than that in Fig. 10c, which is replotted for comparison as the dashed line in Fig. 11c.

CONCLUSION

This paper has presented a method for designing high performance echo-planar spin-echo pulses. Although designed for a blipped echo-planar trajectory, they work well as spectral-spatial (or continuous echo-planar) pulses. As spectral-spatial pulses there is some distortion in the profile which increases with the distance from the designed zero frequency, as well as additional "ghost" sidelobes. This distortion can be eliminated at one frequency by setting that frequency to zero in the pulse design. For cases where the spectral profile will be resolved, a substantial improvement in profile can be obtained by going to a minimum-phase spectral design.

ACKNOWLEDGMENT

The authors thank the GE Medical Systems Group for their help and support.

REFERENCES

1. P. Mansfield, Multi-planar image formation using NMR spin echos. *J. Phys. C.: Solid State Phys.* **10,** L55 (1977).
2. C. H. Meyer, J. M. Pauly, A. Macovski, D. Nishimura, Simultaneous spatial and spectral selective excitation. *Magn. Reson. Med.* **15,** 287 (1990).
3. D. Spielman, J. Pauly, A. Macovski, D. Enzmann, Spectroscopic imaging with multi-dimensional pulses for excitation: SIMPLE. *Magn. Reson. Med.* **19,** 67 (1991).
4. D. M. Spielman, J. M. Pauly, A. Macovski, G. H. Glover, D. R. Enzmann, Lipid-suppressed single- and multisection proton spectroscopic imaging of the human brain. *J. Magn. Reson. Imaging.* **2(3),** 253 (1992).
5. J. Pauly, D. Nishimura, A. Macovski, A linear class of large-tip-angle selective excitation pulses. *J. Magn. Reson.* **82,** 571 (1989).
6. S. Conolly, J. Pauly, D. Nishimura, A. Macovski, Two dimensional selective adiabatic pulses. *Magn. Reson. Med.* **24(2),** 302 (1992).
7. J. Pauly, D. Nishimura, A. Macovski, Analytic design of large-tip-angle multidimensional pulses. *In* "Proceedings, 8th Annual Meeting, Society of Magnetic Resonance in Medicine, 1989," p. 86.
8. J. Pauly, D. Nishimura, A. Macovski, A *k*-space analysis of small tip excitation. *J. Magn. Reson.* **81,** 43 (1989).
9. S. Conolly, D. Nishimura, A. Macovski, Variable rate selective excitation. *J. Magn. Reson.* **78,** 440 (1988).
10. J. M. Pauly, P. Le Roux, D. Nishimura, A. Macovski, Parameter relations for the Shinnar-Le Roux RF pulse design algorithm. *IEEE Trans. Med. Imaging* **10(1),** 53 (1991).
11. M. H. Buonocore, A Shinnar-Le Roux algorithm for design of 2D and 3D spatially selective RF pulses. *In J. Magn. Reson. Imaging* **2,** 145 (1992).
12. M. Shinnar, J. S. Leigh, The application of spinors to pulse synthesis and analysis. *Magn. Reson. Med.* **12,** 93 (1989).
13. P. Le Roux, Exact synthesis of radiofrequency waveforms. *In* "Proceedings, 7th Annual Meeting, Society of Magnetic Resonance in Medicine, 1988," p. 1049.
14. L. R. Rabiner, B. Gold, *in* "Theory and Application of Digital Signal Processing," Prentice-Hall, Englewood Cliffs, New Jersey, 1975.